CHAPTER IV
RESULTS AND DISCUSSION

4.1 Feed Biodiesel Analysis

In order to determine FAME composition of the feed biodiesel, a gas chromatograph (GC) equipped with a flame ionization detector (FID) was used. The FAMEs composition of feed biodiesel is shown in Table 4.1.

Table 4.1 FAME composition of feed biodiesel

FAME	Structure	%
methyl laurate	C12:0	0.278
methyl myristate	C14:0	1.556
methyl palmitate	C16:0	63.324
methyl stearate	C18:0	4.843
trans-methyl elaidate	*trans*-C18:1	0.127
cis-methyl oleate	*cis*-C18:1	23.636
methyl linoleate	C18:2	4.696
methyl linolenate	C18:3	0.089
methyl behenate	C22:0	0.040

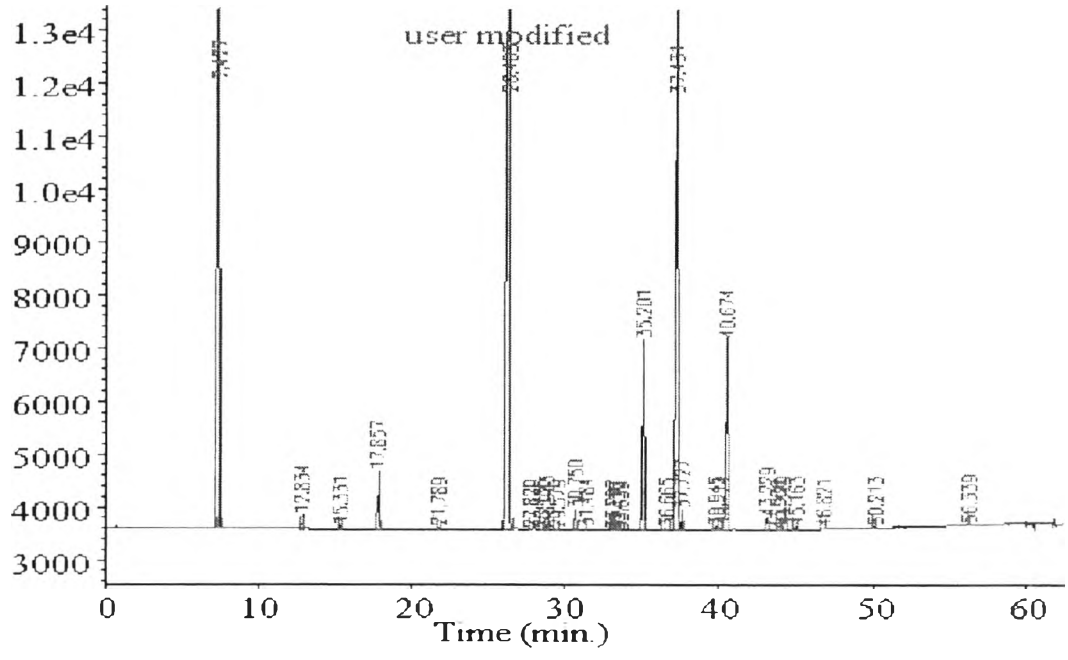

Figure 4.1 Chromatogram of feed biodiesel obtain from gas chromatograph.

4.2 Catalyst Activities for Partial Hydrogenation of Polyunsaturated FAMEs

To study hydrogenation activity of each SiO_2 supported Pd catalysts partial hydrogenation of FAMEs was carried out. The reaction was operated in mild condition of 120 °C, 4 bar, 50 ml/min of hydrogen flow rate, 500 rpm of stirring rate, and 1.5 wt.% of catalyst compared to starting oil.

4.2.1 Effect of Pore Diameter of Silica Support

The effect of pore diameter of silica support on the partial hydrogenation of polyunsaturated FAMEs was studied. The average pore diameters of silica support with difference pore size are shown in Table 4.2.

Table 4.2 Types of silica support

SiO_2 support	Q-3	Q-10	Q-30	Q-50
Average pore diameter (nm)	3	10	30	50
Particle sizes (μm)	180-500	75-500	75-500	200-500

The catalytic activity of these catalysts was identified by FAME composition in the partial hydrogenated biodiesel. FAMEs composition obtain after the partial hydrogenation reaction using Pd/SiO_2 (Q3) as a catalyst, the FAMEs composition is shown in Figure 4.2(a), It was shown that C18:3 decreased from 0.09% to 0% and C18:2 decreased from 4.70% to 0.16% after 4 h of reaction time. The level of *cis*-C18:1 steadily decreased from 23.64% to 4.81%, whereas *trans*-C18:1 initially increased first, then leveled off to 10.08%. Initially, C18:0 content was 4.84% and steadily increased to final value of 18.40% after 4 h of reaction. For the partial hydrogenation reaction by using Pd/SiO_2 (Q10) as a catalyst, the FAMEs composition is shown in Figure 4.2(b); C18:3 decreased from 0.09% to 0% after 2 h of reaction and C18:2 decreased from 4.70% to 0.01%, whereas *cis*-C18:1 rapidly decreased from 23.64% to 0.06%. Then *trans*-C18:1 has 0.13% up to 4.64% in 0.5 h of reaction and decreased to 0.03%. Composition of C18:0 rapidly increased from 4.84% to 33.35% until the end of reaction. Next is the partial hydrogenation reaction by using Pd/SiO_2 (Q30) as a catalyst, the FAMEs composition is shown in Figure 4.2(c); C18:3 also decreased to 0% after 2 h of reaction as same as Pd/SiO_2 (Q10) and C18:2 decreased from 4.70% to 0.01%, whereas *cis*-C18:1 rapidly decreased from 23.64% to 0.04% and *trans*-C18:1 has 0.13% up to 5.15% in 0.5 h of reaction. Then *trans*-C18:1 steadily decreased to 0.02%. Composition of C18:0 rapidly increased from 4.84% to 34.0% in 4 h of reaction. And the last, partial hydrogenation reaction by using Pd/SiO_2 (Q50) as a catalyst, the FAMEs composition is shown in Figure 4.2(d); C18:3 decreased from 0.09% to 0% after 3 h of reaction and C18:2 decreased from 4.70% to 0% until the end of reaction, whereas *cis*-C18:1 steadily decreased from 23.64% to 0.06%. Then *trans*-C18:1 has 0.13% up to 8.80% in 0.5 h

of reaction and leveled off to 0.04%. Composition of C18:0 rapidly increased from 4.84% to 34.90% until 4 h of reaction.

According to these results, it can be concluded that the activity of catalysts in term of complete hydrogenation were found to be in the order of Pd/SiO_2 (Q10) > Pd/SiO_2 (Q30) > Pd/SiO_2 (Q50) > Pd/SiO_2 (Q3). Because silica were mesoporous structure, which have pore diameter between 2-50 nm in case of Pd/SiO_2 (Q3) was too small so FAME composition can't inside on the other side, Pd/SiO_2 (Q50) was too big so FAME can get inside the pore but the reactivity of FAME has limited. Pd/SiO_2 (Q10) was optimum accessibility of FAME to reacts with palladium in pore.

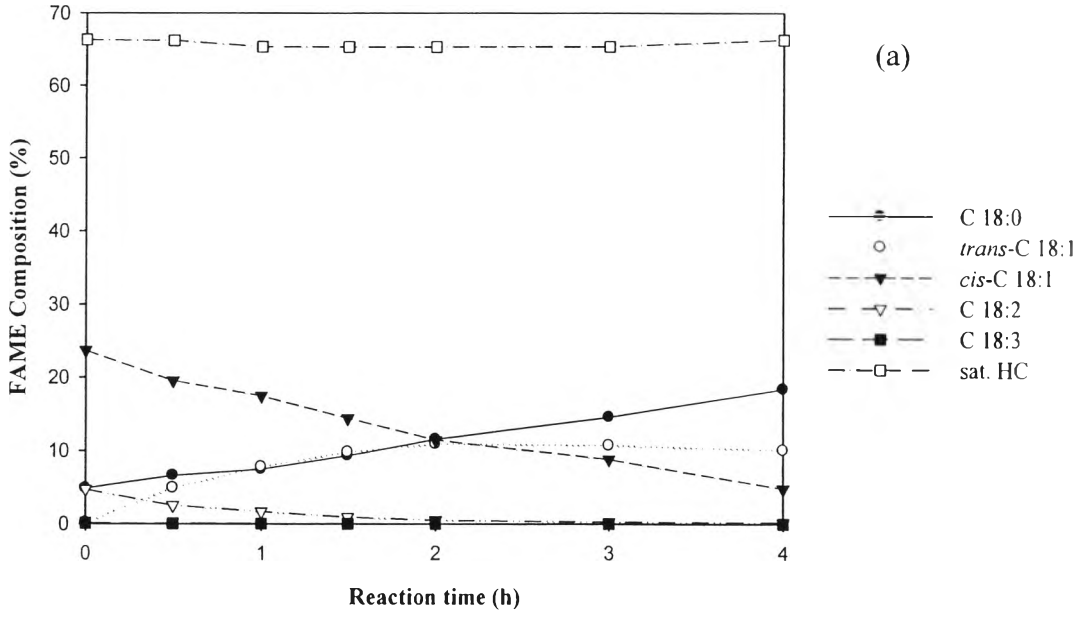

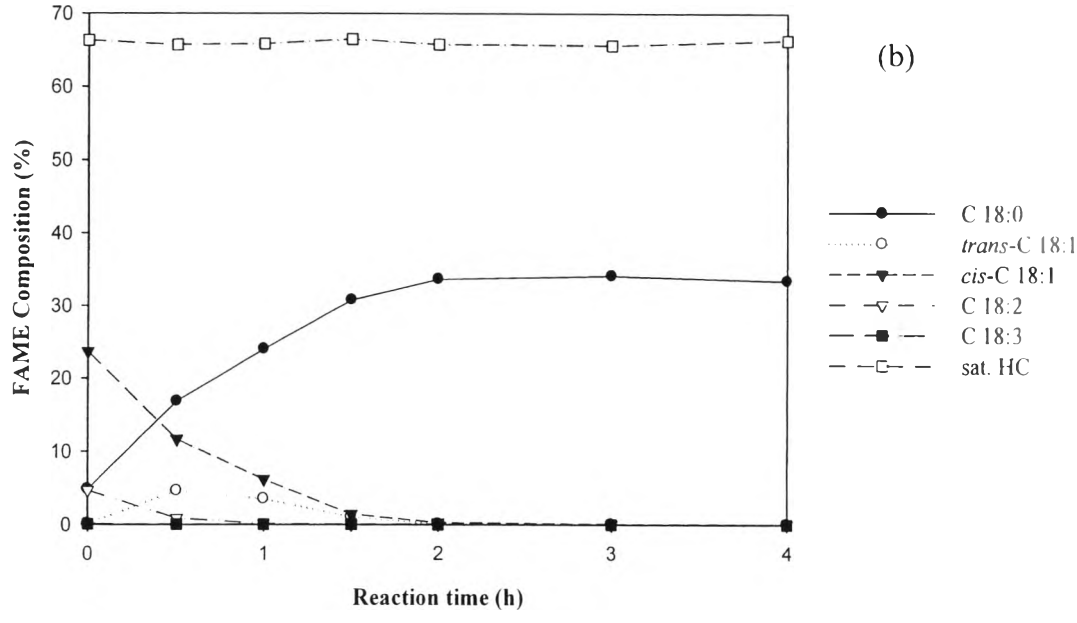
(b)
FAME Composition (%)
Reaction time (h)
C 18:0
trans-C 18:1
cis-C 18:1
C 18:2
C 18:3
sat. HC

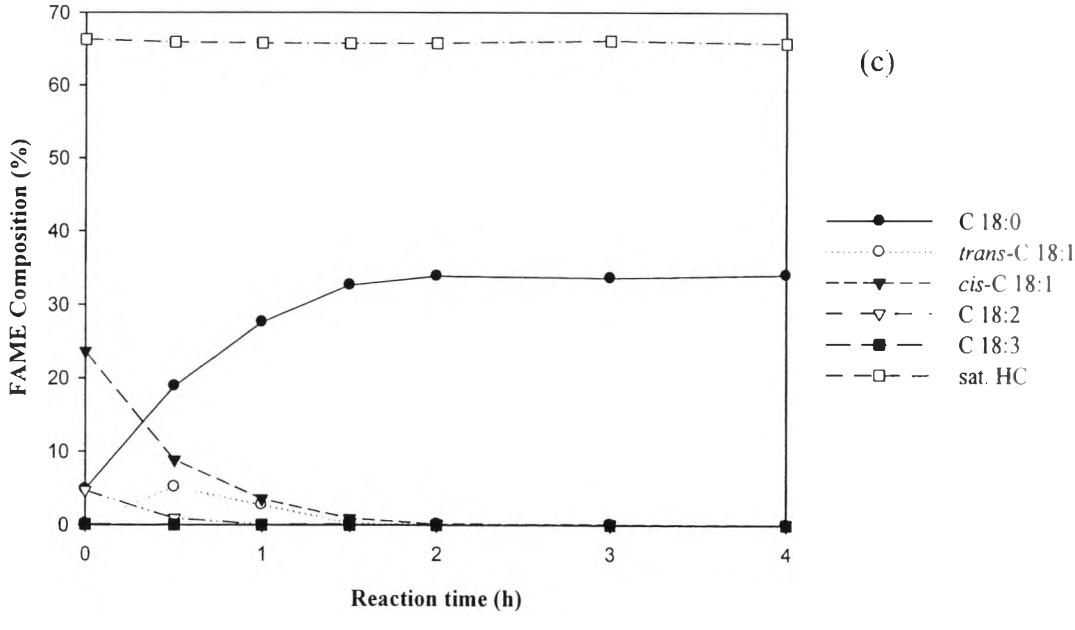
(c)
FAME Composition (%)
Reaction time (h)
C 18:0
trans-C 18:1
cis-C 18:1
C 18:2
C 18:3
sat. HC

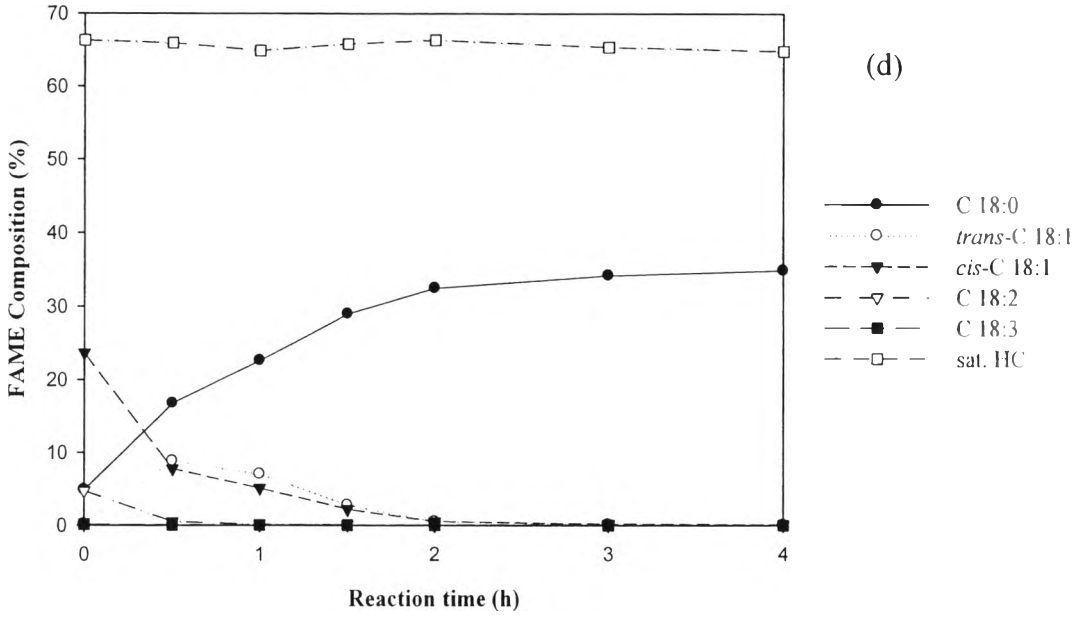

Figure 4.2 Effect of pore diameter of silica support: (a) Pd/SiO_2 Q3 (3 nm, 180-500 μm) (b) Pd/SiO_2 Q10 (10 nm, 75-500 μm) (c) Pd/SiO_2 Q30 (30 nm, 75-500 μm) (d) Pd/SiO_2 Q50 (50 nm, 200-500 μm) on FAME composition of biodiesel after partial hydrogenation reaction using 2 wt.% Pd/SiO_2 (reaction condition: 120 °C, 4 bar, 50 ml/min of H_2 flow rate, 500 rpm of stirring rate, and 1.5 wt.% of catalysts compared with starting oil).

Hydrogen chemisorption technique, which measurements were carried out in a reduction step, which samples were reduced with hydrogen at 250 °C under atmospheric pressure for 3 h. And the amount of hydrogen could be adsorbed at 70 °C. Table 4.3 shows % Pd dispersion and turnover of frequency (TOF) of 2 wt.% Pd/SiO_2 (Q3, Q10, Q30, and Q50) catalysts, it suggested that the smaller particle sizes of silica support absorb less hydrogen than the larger ones so the % Pd dispersion in order from Pd/SiO_2 (Q3) < Pd/SiO_2 (Q10) < Pd/SiO_2 (Q30) < Pd/SiO_2 (Q50). The turnover of frequency (TOF) was calculated based on the hydrogen chemisorption data, which resume that Pd/SiO_2 (Q10) > Pd/SiO_2 (Q30) > Pd/SiO_2 (Q50) > Pd/SiO_2 (Q3). The turnover of frequency (TOF) means the amount of reaction occur per number of active site per time, therefore Pd/SiO_2 (Q10) was the

optimum pore size which presented highest activity when compare with the other catalysts at the same Pd loading.

Table 4.3 % Pd dispersion and turnover of frequency (TOF) of 2 wt.% Pd/SiO_2 (Q3, Q10, Q30, and Q50) catalysts

Pd/SiO_2	% Pd dispersion	TOF (h^{-1})
Q3	40	91.88
Q10	43	127.45
Q30	45	123.55
Q50	50	110.27

The X-ray diffraction patterns of fresh and spent 2 wt.% Pd/SiO_2 catalysts are shown in Figure 4.3 and 4.4. These catalysts were prepared by incipient wetness impregnation (IWI) using $Pd(NO_3)_2.2H_2O$ precursor. The diffraction features at Bragg angles of 40.05° and 46.9° for the reduced Pd corresponding to the Pd (111) and (200) planes, respectively (Han *et al.*, 2004). The main characteristic peak after reduction of crystalline Pd plane (111) at 2θ of 40.05°, which is palladium metal (Pd^0) was observed for all Pd/SiO_2 catalysts (Q3, Q10, Q30, and Q50). The mean particle size of Pd was calculated from the full width at half maximum of the Pd (111) diffraction peak at 2θ = 40.05° by applying Scherrer's equation (Somboonthanakij *et al.*, 2007).

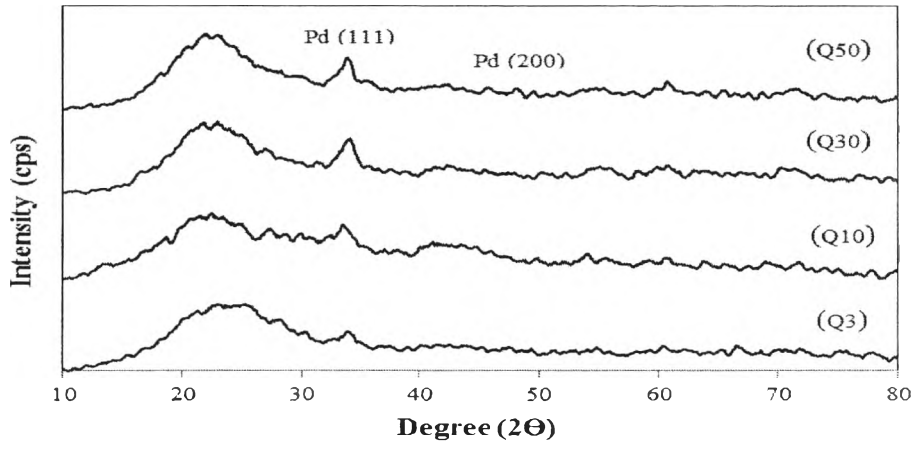

Figure 4.3 XRD patterns of fresh (after calcination step) 2 wt.% Pd/SiO_2 catalysts (a) Q3, (b) Q10, (c) Q30, and (d) Q50.

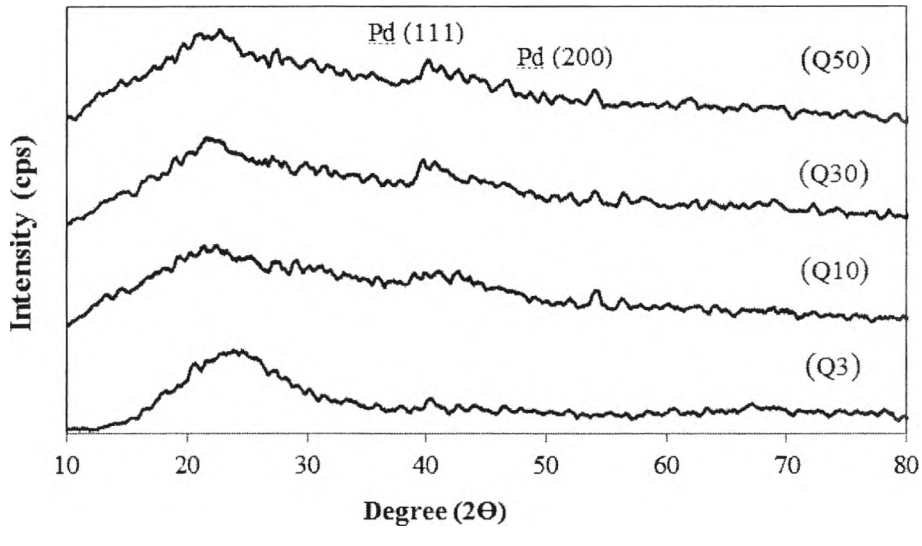

Figure 4.4 XRD patterns of fresh (after reduction step) 2 wt.% Pd/SiO_2 catalysts (a) Q3, (b) Q10, (c) Q30, and (d) Q50.

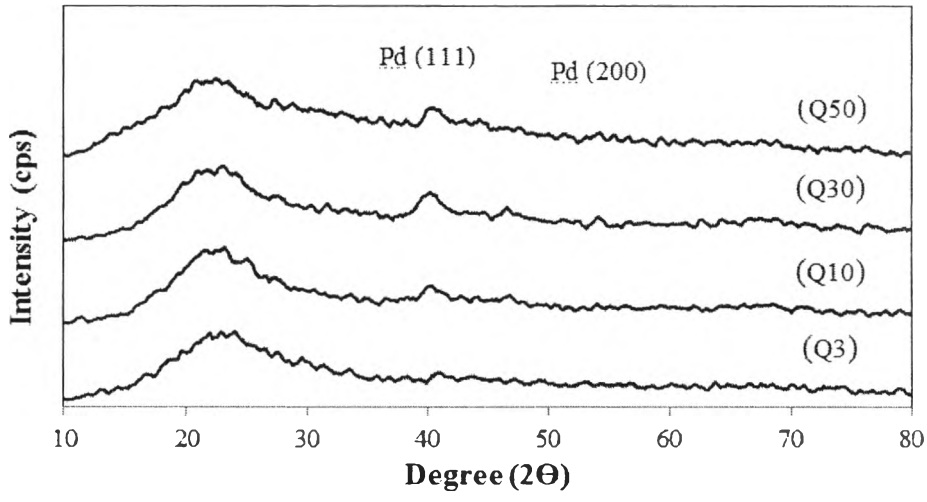

Figure 4.5 XRD patterns of spent 2 wt.% Pd/SiO_2 catalysts (a) Q3, (b) Q10, (c) Q30, and (d) Q50.

Table 4.4 Pd particle size of 2 wt.% Pd/SiO_2 catalysts: Q3, Q10, Q30, and Q50 obtained from XRD technique by applying Scherrer's equation

Pd/SiO_2 Catalysts	**Pd particle size [(111)], nm**	
	Fresh	**Spent**
Q3	6.32	7.68
Q10	5.32	5.54
Q30	5.99	6.66
Q50	6.29	7.26

The Pd particle sizes of Pd/SiO_2 (Q3, Q10, Q30, and Q50), which were calculated by applying Scherrer's equation are reported in Table 4.4. After calcination at 500 °C and 3 h, the diffraction peaks for Palladium oxide (PdO) were detectable at 33.5°. After reduction and reaction, Palladium metal (Pd^0) was in evidence with diffraction peaks at 40.05° so we need to reduce catalyst before partial hydrogenation reaction to change Palladium oxide (PdO) form to Palladium metal

(Pd^0), which active form for hydrogenation reaction. In fresh catalysts, the Pd^0 particle sizes Pd/SiO_2 (Q3), Pd/SiO_2 (Q10), Pd/SiO_2 (Q30), and Pd/SiO_2 (Q50) were found to be 6.32 nm, 5.32 nm, 5.99 nm and 6.29 nm, respectively. The Pd^0 particle sizes of the fresh catalysts were in order of Pd/SiO_2 (Q10) > Pd/SiO_2 (Q30) > Pd/SiO_2 (Q50) > Pd/SiO_2 (Q3), these results related to the hydrogenation activity and suggested that SiO_2 (Q10) was the optimum pore size for the accessibility of FAME to reacts inside the pore with Pd sites due to Pd particle sizes of Pd/SiO_2 (Q3) was bigger than the pore so Pd particle sizes can be located only at surface area and also get lowest hydrogenation activity too. The Pd^0 particle size of spent Pd/SiO_2 (Q3), Pd/SiO_2 (Q10), Pd/SiO_2 (Q30), and Pd/SiO_2 (Q50) catalysts were found 7.68 nm, 5.54 nm, 6.66 nm and 7.26 nm, respectively. After reaction, it was found that Pd particle sizes of all spent catalysts became larger, which was suggesting a sintering of palladium metal particles (Panpranot *et al.*, 2004).

The BET surface area and total pore volume of SiO_2 support and Pd/SiO_2 (Q3, Q10, Q30, and Q50), which were analyzed by using Autosorb-1 surface area analyzer are given in Table 4.5 and 4.6. It was found that, after impregnation of palladium, the BET surface area were smaller. The BET surface area were following order: Pd/SiO_2 (Q3) > Pd/SiO_2 (Q10) > Pd/SiO_2 (Q30) > Pd/SiO_2 (Q50). Pd/SiO_2 (Q3) showed the highest surface area of 700.0 m^2/g, suggested that small pore size shows a higher surface area. The BET surface areas of all supports were decreased from those of the original support to 208.0 m^2/g, 274.9 m^2/g, 107.1 m^2/g and 66.1 m^2/g, respectively. It can suggest that palladium was deposited in some of the pores of the supports (Tiengchad *et al.*, 2010). In Table 4.6 shown the average pore diameter also showed the nearly values when compare with the average pore diameter from catalogs.

Table 4.5 Surface area and total pore volume of SiO_2 (Q3, Q10, Q30, and Q50) and Pd/SiO_2 catalysts from Autosorb-1 surface area analyzer

Pd/SiO_2 Catalysts	**Surface area (m^2/g)**		**Total pore volume (ml/g)**
	SiO_2 Support	**Pd/SiO_2**	
Q3	700.0	208.0	0.355
Q10	281.1	274.9	1.305
Q30	112.1	107.1	1.233
Q50	69.34	66.1	1.226

Table 4.6 Average pore diameter of SiO_2 (Q3, Q10, Q30, and Q50) from catalogs and Autosorb-1 surface area analyzer

SiO_2	**Q3**	**Q10**	**Q30**	**Q50**
Average Pore Diameter (nm)	3	10	30	50
Average Pore Diameter (nm) Analyzed from BET AS-1	2.632	16.71	43.28	66.27

4.2.2 Effect of Percentage of Palladium Loading

In this section, the effects of percentage of palladium loading: 1 wt.% and 2 wt.% on silica (Q10, Q30, and Q50) supports on the partial hydrogenation of polyunsaturated FAMEs were studied. Pd/SiO_2 (Q3) didn't concern in this effect because Pd/SiO_2 (Q3) still have high composition of unsaturated fatty acid consist of

C18:3 and C18:2 and also shown lowest hydrogenation activity. The catalytic activity of these catalysts was indicated by examining FAME composition in the partial hydrogenation of biodiesel. For the partial hydrogenation reaction using Pd/SiO_2 (Q10) as a catalyst, the FAMEs composition is shown in Figure 4.6(a), It was shown that C18:3 decreased from 0.09% to 0% and C18:2 decreased from 4.70% to 0.02% after 4 h of reaction time. The level of *cis*-C18:1 steadily decreased from 23.64% to 0.57%, whereas *trans*-C18:1 initially increased first, then leveled off to 0.25%. Thus C18:0 content remain low at 4.84% but steadily increased to final values at 33.43% after 4 h of reaction. And the partial hydrogenation reaction by use Pd/SiO_2 (Q30) as a catalyst, the FAMEs composition is shown in Figure 4.6(b); C18:3 decreased from 0.09% to 0% after 3 h of reaction and C18:2 decreased from 4.70% to 0.02%, whereas *cis*-C18:1 rapidly decreased from 23.64% to 0.23%. Then *trans*-C18:1 has 0.13% up to 9.35% in 0.5 h of reaction and decreased to 0.15%. Composition of C18:0 rapidly increased from 4.84% to 33.84% until the end of reaction. Next is the partial hydrogenation reaction by use Pd/SiO_2 (Q50) as a catalyst, the FAMEs composition is shown in Figure 4.6(c); C18:3 also decreased to 0% after 3 h of reaction as same as Pd/SiO_2 (Q30) and C18:2 decreased from 4.70% to 0.02%, whereas *cis*-C18:1 rapidly decreased from 23.64% to 0.25% and *trans*-C18:1 has 0.13% up to 10.03% in 1.0 h of reaction. Then *trans*-C18:1 steadily decreased to 0.19%. Composition of C18:0 rapidly increased from 4.84% to 33.53% in 4 h of reaction. The order of hydrogenation activity 1 wt.% of Pd/SiO_2 catalysts shown the same trended as 2 wt.% of Pd/SiO_2 catalysts, which were following order Pd/SiO_2 (Q10) > Pd/SiO_2 (Q30) > Pd/SiO_2 (Q50), respectively.

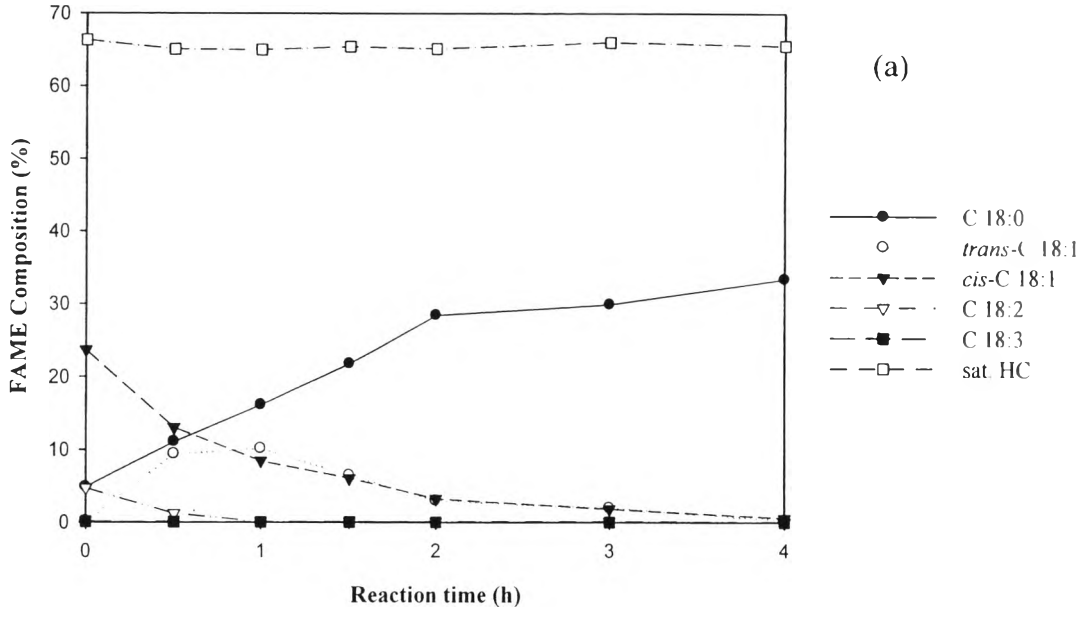
(a)
FAME Composition (%)
Reaction time (h)
C 18:0
trans-C 18:1
cis-C 18:1
C 18:2
C 18:3
sat. HC

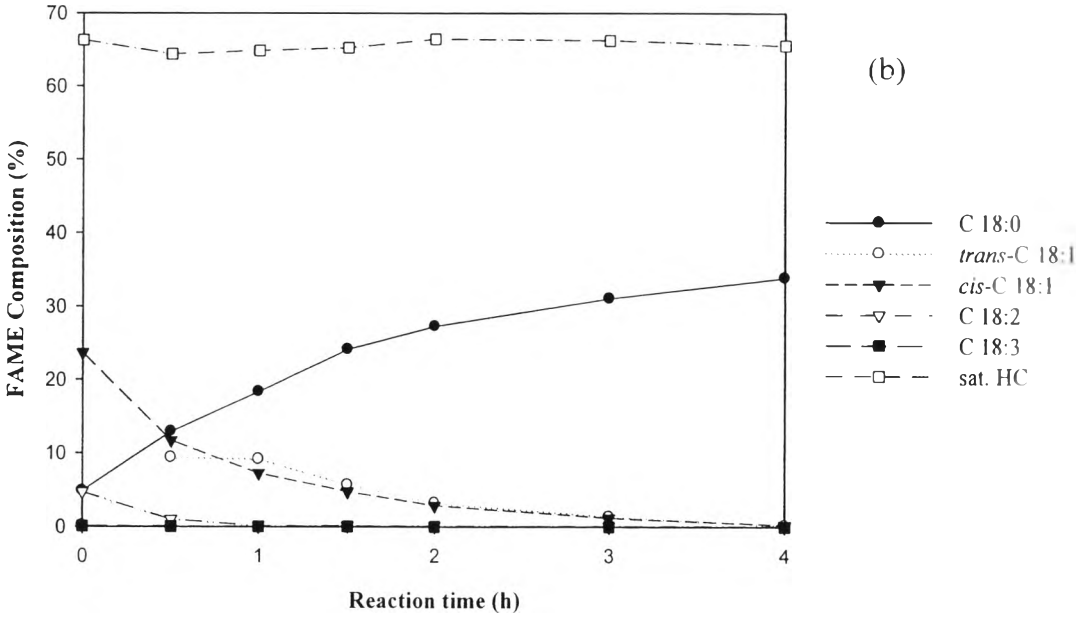
(b)
FAME Composition (%)
Reaction time (h)
C 18:0
trans-C 18:1
cis-C 18:1
C 18:2
C 18:3
sat. HC

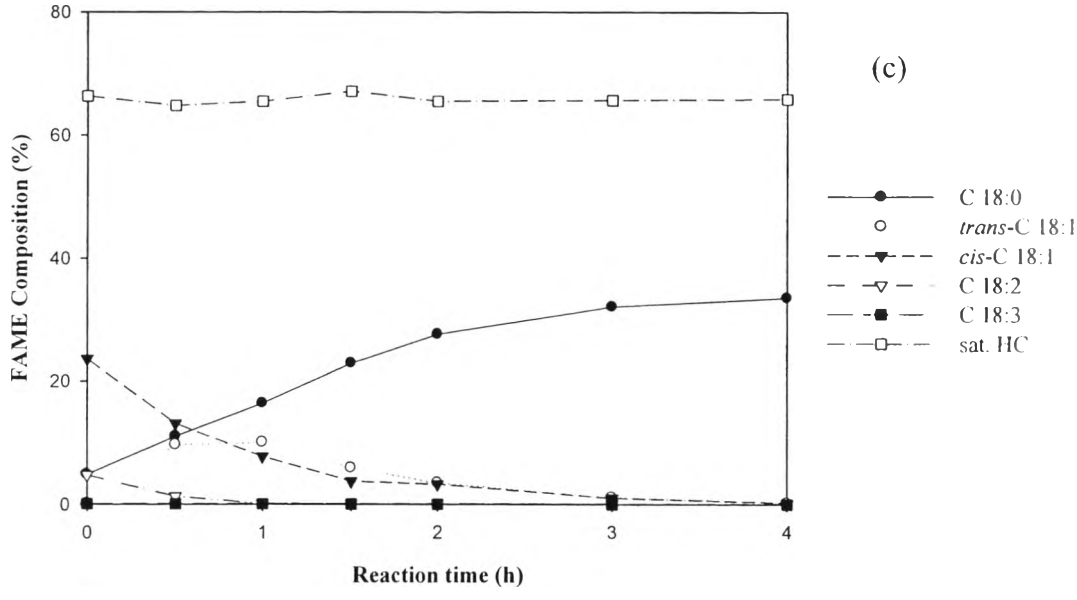

Figure 4.6 Effect of percentage of palladium loading of silica support: (a) Q10 (10 nm, 75-500 μm) (b) Q30 (30 nm, 75-500 μm) (c) Q50 (50 nm, 200-500 μm) on FAME composition of biodiesel after partial hydrogenation reaction using 1 wt.% Pd/SiO_2 (reaction condition: 120 °C, 4 bar, 50 ml/min of H_2 flow rate, 500 rpm of stirring rate, and 1.5 wt.% of catalysts compared with starting oil).

Figure 4.7 shows C18 FAMEs composition of feed and product biodiesel after 1 h of partial hydrogenation using 1 wt.% compare 2 wt.% Pd/SiO_2 (Q3, Q10, Q30, and Q50) catalysts. It was shown that 2 wt.% Pd/SiO_2 catalysts decrease higher amount of polyunsaturated fatty acid methyl esters (C18:3 and C18:2) than 1 wt.% Pd/SiO_2 catalysts when compare with the same time. According to these results, it can be concluded that the hydrogenation activity of 2 wt.% Pd/SiO_2 catalysts were greater than those of 1 wt.%. Since the main purpose of partial hydrogenation is to remove polyunsaturated fatty acid methyl esters (C18:3 and C18:2) with increasing of saturated fatty acid (C18:0), therefore, the 2 wt.% Pd/SiO_2 catalysts were the suitable catalyst, which can convert higher amount of polyunsaturated fatty acid methyl esters as shown in the lower C18:3 and C18:2 than those of 1 wt.%.

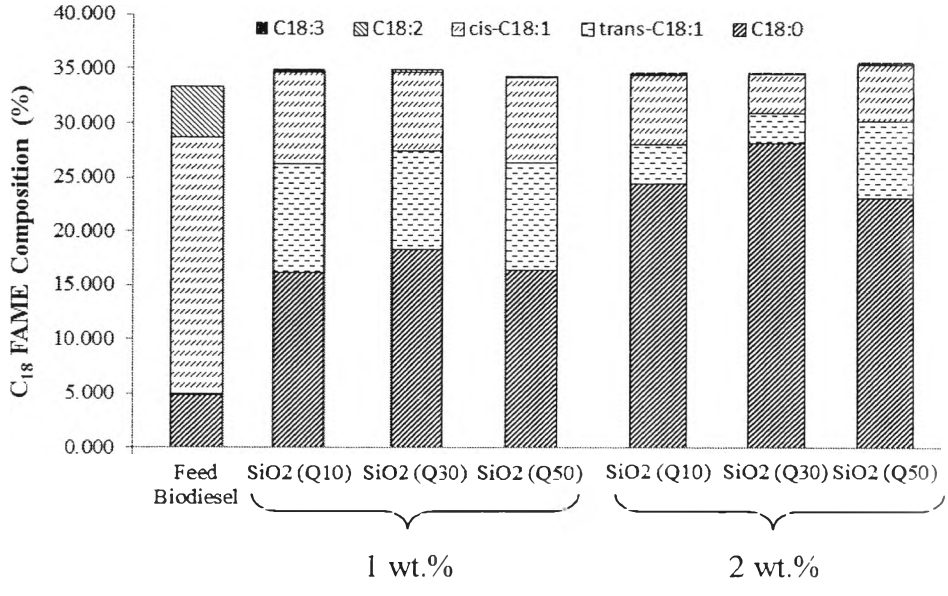

Figure 4.7 C18 FAMEs composition of feed and product biodiesel after 1 h of partial hydrogenation using 1 wt.% compare 2 wt.% Pd/SiO_2 (Q3, Q10, Q30, and Q50) catalysts.

The Atomic Absorption Spectroscopy (AAS) was used to determine the actual amount of palladium on Pd/SiO_2 (Q3, Q10, Q30, and Q50) catalysts, which was prepared by Incipient Wetness Impregnation (IWI) method using $Pd(NO_3)_2.2H_2O$ precursor. In this work, 2 wt.% and 1 wt.% Pd was loaded on the silica support. The percentage of actual Pd loading on each types of silica support is shown in Table 4.7

Table 4.7 The percentage of actual Palladium on Pd/SiO_2 (Q3, Q10, Q30, and Q50) catalysts

Pd/SiO_2 Catalysts	Actual Palladium (wt.%)	
	1 wt.%	2 wt.%
Q3	-	2.10
Q10	1.03	2.07
Q30	1.05	2.05
Q50	1.08	2.02

The X-ray diffraction patterns of fresh and spent 1 wt.% Pd/SiO_2 catalysts are shown in Figure 4.8 and 4.9 in range of 10 - 80°. All the exhibited three characteristic Bragg peaks (Reflection 111, 200 and 220) was observed for Pd/SiO_2 (Q10, Q30, and Q50) catalysts. Figure 4.10 shown the characteristic XRD patterns after calcination step in Pd plane (111) at 2θ of 40.05°. The mean particle size of Pd was calculated from the peak width at half height of the Pd (111) diffraction peak by applying Scherrer's equation (Somboonthanakij *et al.*, 2007).

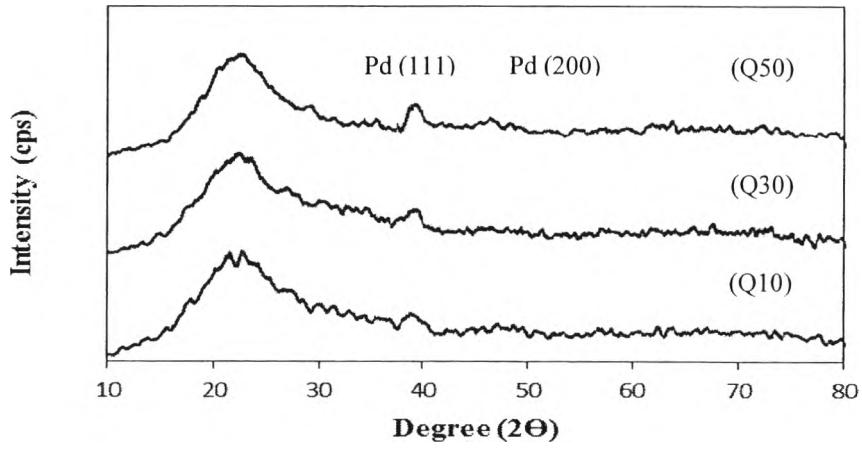

Figure 4.8 XRD patterns of fresh (after reduction step) 1 wt.% Pd/SiO_2 catalysts (a) Q10, (b) Q30, and (c) Q50.

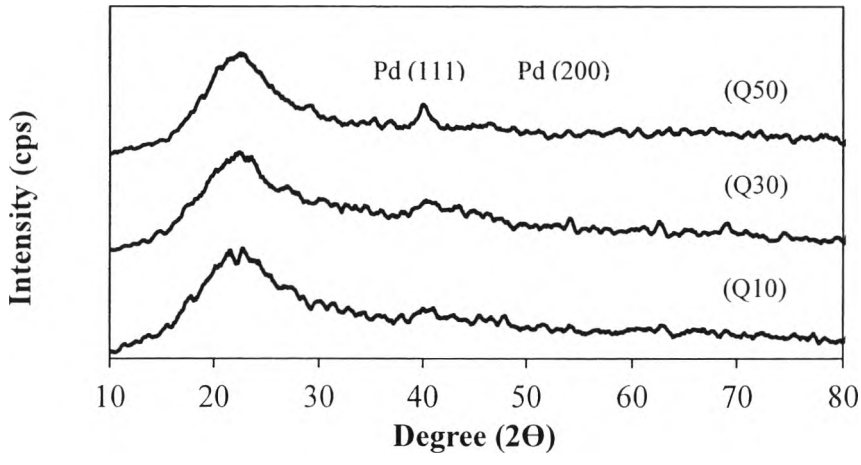

Figure 4.9 XRD patterns of spent 1 wt.% Pd/SiO_2 catalysts (a) Q10, (b) Q30, and (c) Q50.

The Pd particle sizes of Pd/SiO_2 (Q10, Q30, and Q50) were calculated by applying Scherrer's equation was reported in Table 4.8. After reduction and reaction, Palladium metal (Pd^0) was in indicated with diffraction peaks at 40.05°. In fresh catalysts, the Pd^0 particles (Q10, Q30, and Q50) were found 3.55 nm, 3.90 nm and 5.99 nm, respectively. The Pd^0 particles (Q10, Q30, and Q50) in spent catalysts were found 4.09 nm, 4.10 nm and 7.45 nm, respectively. After reaction, spent catalysts were found that Pd particle sizes for all catalyst samples became larger, suggesting sintering of palladium metal particles (Panpranot *et al.*, 2004).

Table 4.8 Pd particle size of 1 wt.% Pd/SiO_2 catalysts: Q10, Q30, and Q50 obtained from XRD technique by applying Scherrer's equation

Pd/SiO_2 Catalysts	**Pd particle size [(111)], nm**	
	Fresh	**Spent**
Q10	3.55	4.09
Q30	3.90	4.10
Q50	5.99	7.45

4.2.3 Catalyst Characterization

The characteristics of the catalysts before and after reaction were obtained using various analysis tools. The spent catalysts were collected after 4 h of reaction and dried at 110 °C for 3 h before analysis.

4.2.3.1 Temperature Programmed Reduction (TPR)

The temperature programmed reduction in calcination state of Pd/SiO_2 (Q3, Q10, Q30, and Q50) catalysts as shown in Figure 4.10 and 4.11. According to the results, the TPR profiles of all samples indicated reduction peak approximately at 100-200 °C and the reduction temperature in partial hydrogenation reaction took place at 300 °C, so it's enough to reduce PdO form and no oxidized palladium structures were reduced in temperature range from 200 °C to 900 °C. On the other hand, the TPR profiles of Pd/SiO_2 catalysts show negative peak at 75 °C, which commonly associated with the decomposition of hydride species (Castano *et al.*, 2006).

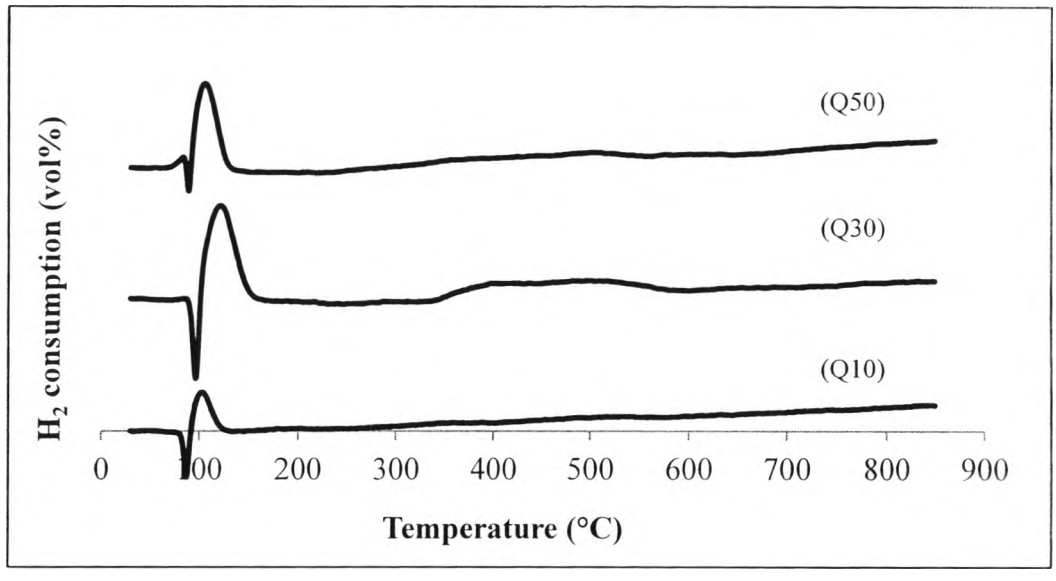

Figure 4.10 TPR profile of calcined 1 wt.% Pd/SiO_2 catalysts: (a) Q10, (b) Q30, and (c) Q50.

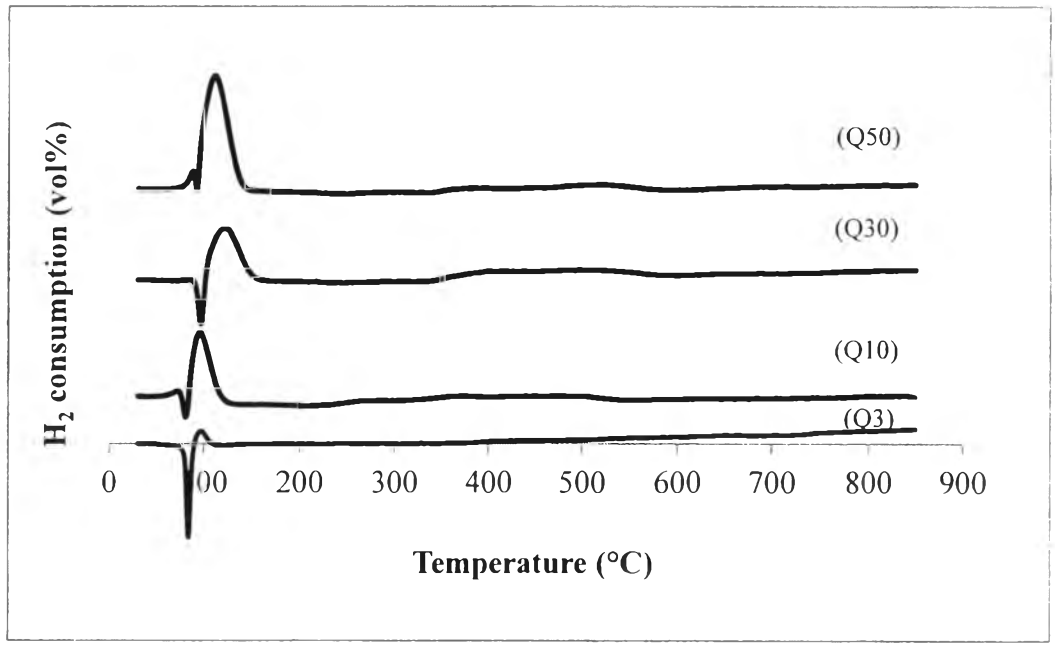

Figure 4.11 TPR profile of calcined 2 wt.% Pd/SiO_2 catalysts: (a) Q3, (b) Q10, (c) Q30, and (d) Q50.

4.2.3.2 Scanning Electron Microscope (SEM)

The temperature SEM micrographs of Pd/SiO_2 (Q3, Q10, Q30, and Q50) catalysts are shown in Figure 4.12. The SEM micrographs shown different catalyst particle sizes. For both Q10 and Q30 supported catalysts, the particles sizes were approximately 75-500 μm, whereas particle sizes of the Q3 and Q50 were around 180-500 μm, respectively.

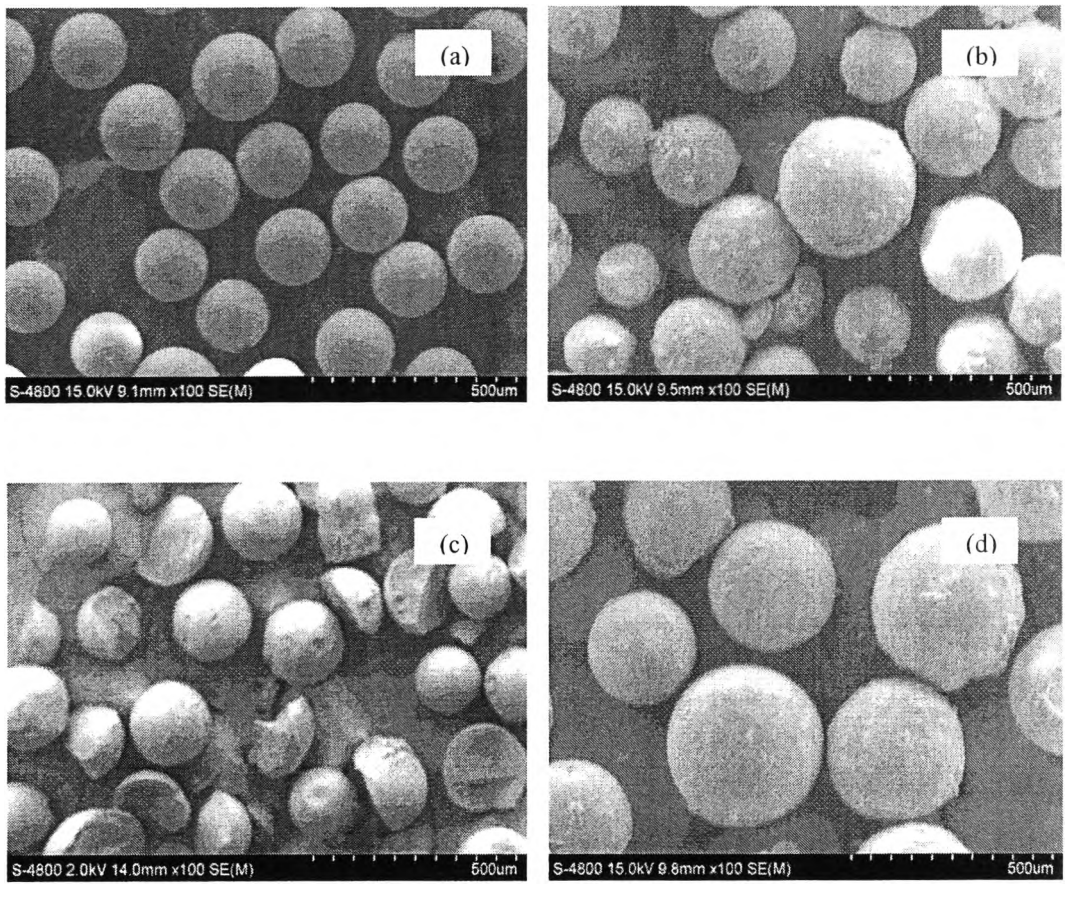

Figure 4.12 SEM micrographs of Pd/SiO_2 catalysts: (a) Q3, (b) Q10, (c) Q30, and (d) Q50.

4.3 Biodiesel Property after Partial Hydrogenation of Polyunsaturated FAMEs

The properties of biodiesel are close to diesel fuels. One of the most important characteristics of biodiesel is oxidative stability therefore this research

needs to improve this property by Rancimat testing (European standard EN14112 method).

4.3.1 Oxidative Stability

Oxidative stability is one of the major issues affecting the use of biodiesel because of its content of polyunsaturated methyl esters (Knothe, 2010). Oxidative stability expresses the susceptibility to oxidation upon exposure to air of biodiesel (Ramos *et al.*, 2009). Oxidative stability of feed biodiesel and biodiesel after partial hydrogenation were shown in Table 4.9. This results shown oxidative stability of biodiesel after partial hydrogenation higher than feed biodiesel. A high oxidative stability guarantees that the biodiesel can be used reliably under conditions of normal use.

Table 4.9 Oxidative stability of feed biodiesel and biodiesel after partial hydrogenation in condition: 2 wt.% Pd/SiO_2 (Q10)

	Feed biodiesel	**Biodiesel after partial hydrogenation**
Oxidative stability (h)	19.21	>72